An investigation into structure of aqueous NaCl electrolyte solutions under magnetic fields

2 AUTHORS, INCLUDING:

Cheng-I Weng
National Cheng Kung University
157 PUBLICATIONS **1,717** CITATIONS

ELSEVIER

An investigation into the electrical properties of finite carbon nanotubes in the presence of polar molecules

Yi-Ray Chen [a], Cheng-I Weng [a,b,*]

[a] *Department of Mechanical Engineering, National Cheng Kung University, Tainan, Taiwan, ROC*
[b] *Fo Guang University, Jiaushi, IIan County, Taiwan, ROC*

Abstract

This study employs quantum transport theory to investigate the electrical properties of zigzag carbon nanotubes with different hopping integrals. It is found that the current-bias voltage profiles have a step-like form, in which each step corresponds to the voltage bias at which the energy imparted to the electrons is sufficient to cause them to hop between neighboring atoms. In carbon nanotubes with a length of several nanometers, the normalized-current-voltage profiles exhibit prominent peaks as the hopping integral decreases and distinct troughs as the hopping integral increases. In longer nanotubes, the current changes by several orders of magnitude in these peak and trough regions of the current–voltage curves. Furthermore, the peaks and troughs appear at lower values of the bias voltage. The results presented in this study suggest that semi-conducting zigzag nanotubes with an appropriate bias have the potential for use as ion or polar molecule absorption sensors.
© 2007 Elsevier B.V. All rights reserved.

Keywords: Semi-conducting zigzag carbon nanotube; Tunnelling transport; Polar molecules absorption sensor

1. Introduction

Conventional Si-based electronic components are no longer feasible when the widths of the conducting wires are less than 80 nm. At such small scales, the behavior of the system can be understood by applying the principles of quantum mechanics theory. Many of today's electronic components exploit quantum effects, including tunneling field-effect transistors and single-electron transistors. Furthermore, nanoscale electrical components consisting of just several atoms or molecules have an exciting potential for use in a range of industrial applications.

Electrical transport in single-walled carbon nanotubes (SWNTs) [1–5] has attracted significant interest in recent years. Many simulation-based studies have investigated the potential to exploit the unique nanometer scale and electronic properties of SWNTs to develop nanoscale electronic devices. Carbon nanotubes are suitable for a broad range of applications. However, in terms of their use as electronic devices, nanotubes can be regarded as one-dimensional "quantum wires", which may be either semi-conducting or metallic depending on their chiral vector [6]. In the way of electrical transport in molecules, Yibin et al. [7] presented the *I–V* characteristics of 4,4′bipyridine and 6-alkanedithiol between Au electrodes, while Fagas et al. [8] discussed electrical transport in a molecular wire connecting two semi-infinite carbon nanotube leads (known as nano-electrodes). Ke et al. [9] analyzed the conductance of molecules by evaluating the gate-induced polarizations and the potential shift of the molecules.

The transport characteristics of SWNTs render them suitable for gas and fluid sensing applications. Kong et al. reported that the absorption of gaseous molecules such as NO_2 or NH_3 on the surface of a semi-conducting

* Corresponding author. Address: Department of Mechanical Engineering, National Cheng Kung University, Tainan, Taiwan, Roc. Fax: +886 6 2352973.
E-mail addresses: l98802002@yahoo.com.tw (Y.-R. Chen), weng@mail.ncku.edu.tw (Cheng-I Weng).

SWNT causes a significant change in its electrical resistivity [10]. A similar effect was also observed in SWNTs exposed to hydrogen gas [11]. Accordingly, researchers have investigated other appropriate sensor materials and have proposed a variety of feasible manufacturing technologies [12–14]. Ghosh et al. reported that the voltage across a SWNT bundle varies depending on the velocity of the liquid flowing over its surface [15,16]. In a later study, the same authors used an *ab initio* method to calculate the variation of the strain and the π–π overlap energy in a nanotube exposed to ions [17].

The literature of polar molecules contains many theoretical investigations into nanoscale detectors. Jijun et al. [18] used a first principles method to study the absorption of various gas molecules on the surfaces of individual SWNT and SWNT bundles, respectively. The results revealed that the density of state (DOS) of a nanotube with a single absorbed NH_3 molecule on its surface was very similar to that of a pure nanotube. Furthermore, the charge transfer from the molecule to the nanotube is very little, and hence there is almost no effect on the electronic transport properties. Also, Na et al. [19] showed that the charge transfer decreased as the number of water molecules around a nanotube increased. These studies revealed that the charge transfer, and hence the effect of the position of the Fermi level was neglected when a large number of molecules are absorbed around the nanotube.

The studies above used either *ab initio* or first principles methods to simulate the absorption of molecules on carbon nanotubes. However, the computational complexity of such methods limits their applicability to systems containing fewer than one hundred atoms. In practical systems, polar molecules do not exist in isolation, but gather in their hundreds or thousands to form clusters. Therefore, computational models that consider the effects of small numbers of molecules are unable to account for the more realistic case in which polar molecules are distributed over the surface of the nanotube. When a molecular cluster wraps itself around the tube, it causes a non-uniform change in the hopping integral (i.e. the ability of electrons to jump from one atom to its neighbor) over the entire tube surface. However, for simplicity, the current analysis assumes that the average hopping integral, t, changes uniformly over the surface.

This study is to investigate the electrical properties of finite carbon nanotubes in the presence of polar molecules (for example: NH_3 or H_2O). The remainder of this paper is organized as follows. Section 2 derives the current-bias voltage relationship for the nanotube. In deriving this formula, the eigenvalues of the end sites of the semi-infinite metallic electrodes are calculated using the tight-binding method, and the interactions between the electrodes and the nanotube are evaluated using the Dyson equation. The tight-binding Hamiltonian of the nanotube and the Green's function represents the *T*-matrix. The current-bias voltage characteristics of the nanotube are calculated via Landauer's formulism. Section 3 presents the results and

discussions. Finally, Section 4 draws some brief conclusions.

2. Theoretical formula derivation

This study uses quantum transport theory to compute the *I–V* characteristics of a finite zigzag carbon nanotube for different values of the hopping integral. As shown in Fig. 1, the analysis assumes that the nanotube is attached at either end to ideal electrodes. In general, zigzag nanotubes $(n,0)$ are metallic when the index n is a multiple of 3, and semi-conducting otherwise. The current analysis is restricted to the case of a semi-conducting (10,0) zigzag nanotube. In such a nanotube, adjacent rings of carbon atoms are referred to as "unit cell" that was shown by the square dash lines in Fig. 1, and the interval between two unit cells is three times the bond length. The nanotubes considered in this study vary in length from 15.6 Å to 41.8 Å, equivalent to 4–10 unit cells, respectively. As indicated in Fig. 1, the chemical energies of the left and right electrodes are μ_1 and μ_2, respectively. Furthermore, an assumption is made that the tunneling transport mechanism is coherent. Consequently, the effects of inelastic transport are neglected. The metallic electrodes are assumed to be semi-infinite chains and to have a weak coupling with the nanotube. Furthermore, the coupling is assumed to exist only at the contacting atoms between the electrodes and the side-heads of the nanotube. Finally, the investigations are based on a tight-binding interaction Hamiltonian.

2.1. Eigenvalues of end sites of semi-infinitely long metallic electrodes

The metallic electrodes attached to the two side-heads of the nanotube are assumed to be semi-infinitely long. The Hamiltonian used to describe these electrodes in a tight-binding representation has the form:
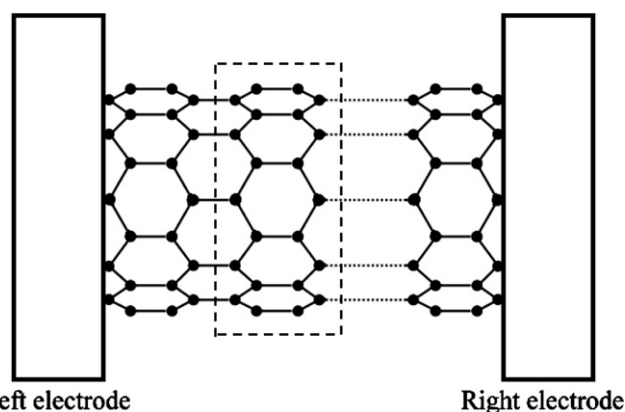

Fig. 1. Schematic illustration of zigzag carbon nanotube between two electrodes. The chemical energies of the left and right electrodes are μ_1 and μ_2, respectively.

$$H = E_0 \sum_n |f_n\rangle\langle f_n| + V_s \sum_n (|f_n\rangle\langle f_{n+1}| + \text{h.c.}), \tag{1}$$

where E_0 is the energy level of the metallic atoms and V_s is the hopping energy between nearest neighboring sites. The bandwidth of the metallic electrodes is equal to $4V_s$. Solving the Green's function of this Hamiltonian yields the eigenvalues of the semi-infinite chain. In the current example, the Green's function of the connecting head of the metallic chain is of interest, i.e. $G(E)_{00}$ in the number index 0. This Green's function has the form:

$$G(E)_{00} = (E - H)^{-1}_{00}. \tag{2}$$

Eq. (2) can be solved recursively using the following relations [20]:

$$G(E)_{00} = \cfrac{1}{E - E_0 - \cfrac{V_s^2}{E - E_0 - \cfrac{V_s^2}{E - E_0 - \cfrac{V_s^2}{\ddots}}}}. \tag{3}$$

In the current case, the bandwidth of the electrodes is very large and hence the recursive expression for $G(E)_{00}$ can be simplified to:

$$G(E)_{00} = \frac{1}{\frac{E-E_0}{2} + i\sqrt{V_s^2 - \left(\frac{E-E_0}{2}\right)^2}}. \tag{4}$$

The pole of $G(E)_{00}$ gives the eigenvalue of the end site of the electrodes.

2.2. Hybridization between electrodes and carbon nanotube

As stated above, the current simulations assume that the metallic electrodes only couple with the nanotube through the tube's end-site atoms. From the Dyson equation, it can be shown that:

$$G(E) = g(E) + g(E)WG(E), \tag{5}$$

where $G(E)$ and $g(E)$ are the interacting and non-interacting Green's functions, respectively, and W is the interaction matrix. Since, the coupling between the electrodes and the nanotube is limited only to the end-site atoms, the atoms involved in the coupling can be classified into two separate groups, i.e. Group A: electrode atoms, and Group B: nanotube atoms. In matrix representation, the Hamiltonian $H = H_0 + W$ describing the coupling system is:

$$\begin{bmatrix} H_{AA} & H_{AB} \\ H_{BA} & H_{BB} \end{bmatrix} = \begin{bmatrix} H_{AA} & 0 \\ 0 & H_{BB} \end{bmatrix} + \begin{bmatrix} 0 & H_{AB} \\ H_{BA} & 0 \end{bmatrix}. \tag{6}$$

Consequently, the effective Hamiltonian, $H_{\text{eff}} = H_{AA} + \Sigma(E)_{AA}$, contains the self-energy:

$$\Sigma(E)_{AA} = \frac{H_{AB}H_{BA}}{E - H_{BB}}, \tag{7}$$

where H_{BB} represents the eigenvalue of the connecting head of the electrode and is derived from the pole of Eq.

(4). Therefore, the self-energies of the connecting heads of the nanotube are given by:

$$\Sigma(E)_{L,R} = \frac{V_e^2}{\frac{E-E_{L,R}}{2} + i\sqrt{V_s^2 - \left(\frac{E-E_{L,R}}{2}\right)^2}}, \tag{8}$$

where $E_{L(R)}$ is the eigenvalue of the left (right) end head of the electrode and is shifted by an applied bias, and V_e is the coupling interaction between the left (right) electrode and the nanotube.

2.3. Tight-binding representation of Hamiltonian of nanotube

In Fig. 1, the nanotube has a finite length and is biased by the left and right electrodes in real space. In this effectively two-dimensional system, the Hamiltonian of the nanotube describing the energies and hopping integrals of the carbon atoms and their interactions with the electrodes has the form:

$$H = \sum_i E_i^m |\phi_i\rangle\langle\phi_i| + \sum_i t_{ij}(|\phi_i\rangle\langle\phi_j| + \text{h.c.}) + \Sigma, \tag{9}$$

where E_i^m is the energy of the ith site. Significantly, the first and final sites contain the self-energies derived above as a result of their interaction with the electrodes. Additionally, t_{ij} is the hopping integral between the ith and the jth sites. The Hamiltonian matrix for the tight-binding representation of the zigzag nanotube is given by:

$$H_{\text{zig}} = \begin{bmatrix} H_R & H_c & 0 & 0 & 0 \\ H_c & \ddots & \ddots & 0 & 0 \\ 0 & \ddots & H_M & \ddots & 0 \\ 0 & 0 & \ddots & \ddots & H_c \\ 0 & 0 & 0 & H_c & H_L \end{bmatrix}, \tag{10}$$

where this matrix is composed of separate sub-matrixes (H_R, H_M and H_L), each representing the Hamiltonian of one individual zigzag ring. H_L and H_R represent the left-hand side and right-hand side zigzag rings, respectively, while H_M represent the zigzag rings between the two ends. t_1 is the hopping integral in real space, and H_c represents the hopping integral between adjacent zigzag rings. The Sub-matrixes can be shown that:

$$H_{R(L)} = \begin{bmatrix} E^m + \Sigma_{R(L)} & t_1 & & & t_1 \\ t_1 & E^m & \ddots & & \\ & \ddots & \ddots & \ddots & \\ & & \ddots & E^m + \Sigma_{R(L)} & t_1 \\ t_1 & & & t_1 & E^m \end{bmatrix}, \tag{11}$$

$$H_{\mathrm{M}} = \begin{bmatrix} E^m & t_1 & & & t_1 \\ t_1 & E^m & \ddots & & \\ & \ddots & \ddots & \ddots & \\ & & \ddots & E^m & t_1 \\ t_1 & & & t_1 & E^m \end{bmatrix}, \qquad (12)$$

$$H_{\mathrm{c}} = \begin{bmatrix} 0 & & & \\ & t_1 & & \\ & & \ddots & \\ & & & 0 & \\ & & & & t_1 \end{bmatrix}. \qquad (13)$$

2.4. Current–voltage formula

In the T-matrix representation, the conductance of the nanotube is given by [21]

$$g = \frac{2\pi e^2}{\hbar} \sum_{i,f} |T_{fi}|^2 \delta(E_i - E_F)\delta(E_f - E_F), \qquad (14)$$

where E_F is the Fermi energy and $T_{fi} = \langle f|T|i\rangle$, with an operator $T = V + VGV$, indicates that the electrons propagate from an initial state $|i\rangle$ to a final state $|f\rangle$ via the coupling interaction, V, and the propagator Green's function, G. As discussed above, the simulations assume that the coupling between the nanotube and the electrodes is restricted to the nanotube head regions. Therefore, it can be shown that

$$\begin{aligned} T_{fi} &= \langle f|V|i\rangle + \langle f|VGV|i\rangle \\ &= \langle f|V|N\rangle\langle N|G|1\rangle\langle 1|V|i\rangle \qquad (15) \\ &= V_{fN}G_{N1}V_{1i}, \end{aligned}$$

where the indexes 1 and N denote the left and right heads of the nanotube, respectively. According to the quantum transport formula, the current induced by the bias voltage, V, is obtained as:

$$I = \frac{2e}{\hbar} \int_{-\infty}^{\infty} dE\, T_{\mathrm{eff}}(E)[f_L(E) - f_R(E + eV)], \qquad (16)$$

where the effective transfer matrix, T_{eff}, is given by $T_{\mathrm{eff}} = (h/e^2)g$ and $f(E)$ is the Fermi–Dirac distribution function. In weak coupling assumption, the current-bias voltage equation can be written as [22,23]:

$$I = 4\frac{2e}{\hbar} \int_{-\infty}^{\infty} dE\, |G_{N1}|^2 \frac{V_e^4}{V_s^2}[f_L(E) - f_R(E + eV)]. \qquad (17)$$

3. Discussion and results

In the present simulations, it is assumed that the weak coupling between the nanotube and the electrodes, V_e, has a value of 0.4 eV, the bandwidth of the electrodes, V_s, is 16.0 eV, and the hopping integral of the carbon nanotube, t, is 3.033 eV. Furthermore, for simplicity, the bias applied to the electrodes is assumed to be symmetrical and to experience no dissipation in contact. Consequently, the biases on the left and right electrodes are $+V/2$ and $-V/2$, respectively. In reality, the applied bias is distributed in accordance with a ratio κ, with a voltage of κV applied to the left electrode, and a voltage of $-(1-\kappa)V$ applied to the right. In the symmetric case assumed in this study, the value of κ is therefore 0.5.

Fig. 2 presents the current-bias voltage profiles for zigzag nanotubes of lengths 4, 6, 8 and 10 unit cells, respec-
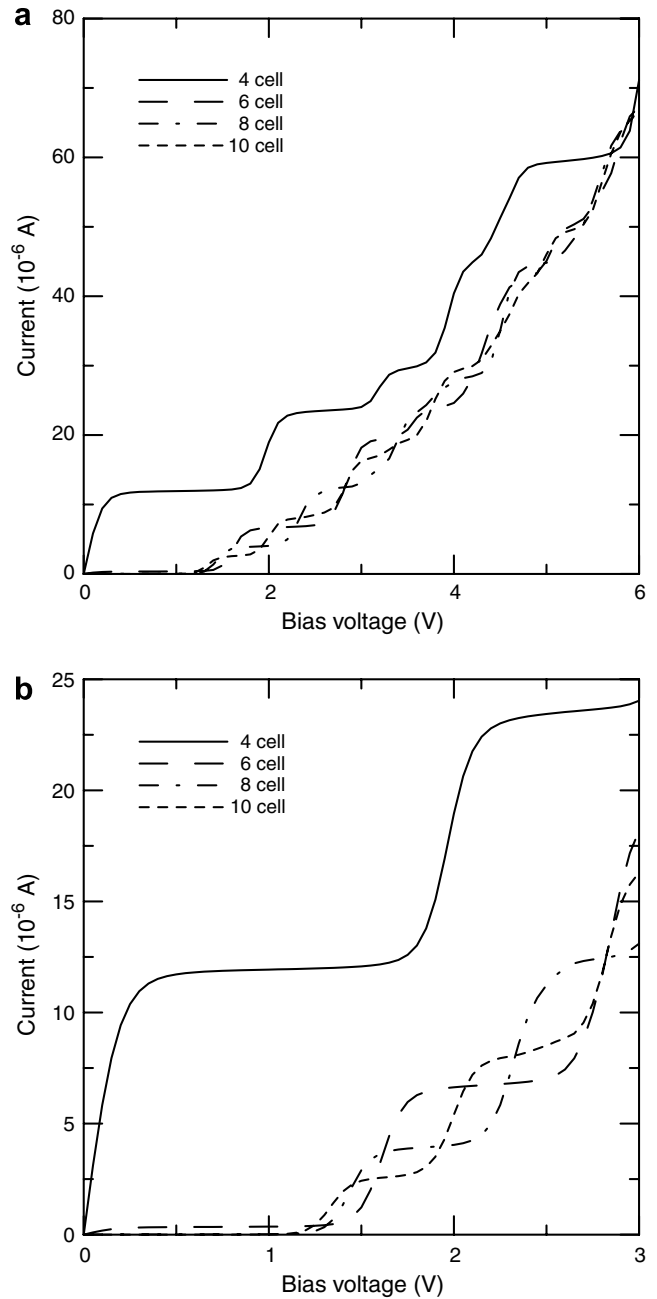

Fig. 2. Variation of current with bias voltage in (10,0) zigzag tubes of different lengths. In (a) the voltage range extends from 0 V to 6 V. (b) provides an enlarged view of (a) in the voltage range 0 V–3 V.

tively. In Fig. 2a, it can be seen that apart from the shortest nanotube (4 unit cells), the *I–V* profiles corresponding to the remaining nanotubes are very close to one another at higher voltages; particularly as the nanotube length increases. Furthermore, it is apparent that the profiles have a step-like appearance and that the number of steps increases with an increasing nanotube length. The steps in the profile correspond to the values of the bias voltage at which the energy applied to the nanotube exceeds the discrete energy states of the tube, and hence cause the electrons to drift from one electrode toward the other in the form of a current. In a short tube, the energy level is composed of a discrete set of energy states as a result of the quantum size effect. However, when the tube has a length of several hundred nanometers or so, the energy level comprises a quasi-continuous energy state, and consequently the steps increase in number but decrease in height to give the impression of a smoother curve. In the arrangement shown in Fig. 1, the nanotube can be regarded as a conductor, and electron transport takes place without scattering and with zero electronic resistance. Therefore, the only resistance, which arises, is that produced at the point of contact between the nanotube and the electrodes. Therefore, the resistance is independent of the lead length, and varies only with the number of transverse modes in the lead. Fig. 2b shows that the current is approximately zero for a bias voltage of less than 1.1 V (corresponding to the energy gap of the (10,0) nanotube) in nanotubes with a length of 6–10 unit cells. This leakage current is due to the tunneling effect and becomes less significant as the nanotube length increases. In general, nanotubes in air become burned when the bias voltage exceeds several tens of volts. Hence, the remaining simulations in this study are restricted to voltages of less than 3 V.

In the Gas-sensing experiments, Kong et al. [10] used a sealed 500-ml glass flask. The diluted NH_3 (0.1–1%) in Ar or air (flow rate of 700 ml/min) flowed through the flask while monitoring the resistance of the tube. They found that the electrical resistance had a significant change. For such a volume; the number of polar molecules is approximately 10^{21}, equivalent to 1 mole. In the experiment, the concentration of the gas molecules is of the order of several percentages, and the number of gas molecules is at least 10^{18}. In practice, polar molecules form clusters with hundreds or thousands of members. So the clusters have the stronger attracting force between the tube and the clusters, and the tube would be wrapped up by the clusters with the number of molecules increasing. Therefore, the results presented in previous studies [18,19] for the absorption of just several molecules on the nanotube surface are unrealistic. Accordingly, the present analysis considers the case where molecules or ions cover the entire surface of the tube. Previous studies have reported a variation in the strain and the π–π overlap energy when a nanotube surface is surrounded by a ring of ions [17]. Dobrokhotov et al. reported a change in the band structure of carbon nanotubes as a result of the presence of a uniformly charged shell [24]. When ions or

polar molecules are absorbed on a nanotube, a change occurs in the π orbital overlap between the nearest neighboring carbon atoms. As a result, the hopping integral between two adjacent $2p_z$ atomic orbitals may either increase or decrease. Although, the hopping integral is not directly accessed by experiments, there exists some relation with that obtained by the features of the optical absorption spectrum. For example, the energy of the second peak in optical absorption spectrum has the form [25]:

$$E_2 = 2\left[\left(\frac{\varepsilon_p^c - \varepsilon_p^a}{2}\right)^2 + \left(\frac{4}{3}V_{pp\sigma} + \frac{8}{3}V_{pp\pi}\right)^2\right]^{1/2}, \tag{18}$$

where ε_p^c and ε_p^a represent the cation and anion energy of p orbital, respectively; $V_{pp\sigma}$ and $V_{pp\pi}$ are the interaction of σ and π band of two p orbitals, respectively. Moreover, the interaction of orbitals s or p varies inversely with the square of the distance (R^{-2}) between the nearest neighboring atoms. The interaction has the following form:

$$V_{\alpha\beta} = V_{\alpha\beta}^0 (R_0/R)^{n_{\alpha\beta}}, \tag{19}$$

where $V_{\alpha\beta}$ and $V_{\alpha\beta}^0$ are the interactions of two orbitals. R and R_0 are the distances between the adjacent atoms, and they are the function of the pressure. Additionally, α and β denote the orbitals s or p, respectively, and $n_{\alpha\beta} = 2$ in accordance with Harrison's law. When the energy of second peak is changed by the pressure, $V_{pp\sigma}$ and $V_{pp\pi}$ can be calculated by Eqs. (18) and (19) mentioned above. When a molecular cluster is wrapped around the tube, the hopping integral changes over the entire tube surface. However, to simplify the current analysis, an assumption is made that the effective hopping integral, t, changes uniformly over the nanotube surface.

Fig. 3a and b plot the current-bias voltage profiles of a zigzag nanotube with a length of 24.5 Å as a function of decreasing and increasing hopping integrals, respectively. Distinct steps are evident in the current-bias curves at particular values of the bias voltage. As discussed previously, these steps coincide with the values of the bias voltage at which the energy imparted by the electrodes exceeds the discrete energy states of the tube. As shown in Fig. 3a, the current increases as the hopping integral decreases. This phenomenon is due to the molecular orbits of the absorbed molecules and the host molecules that hybridize close to one another, resulting in slightly decreasing hopping integral between the carbon atoms. This condition causes the increasing number of discrete energy states at a lower bias voltage. Conversely, as the hopping integral increased, fewer discrete energy states presented at lower values of the bias voltage. For this reason, the current reduces with increasing hopping integral, and the first step in the profile appears at a higher voltage as shown in Fig. 3b.

Fig. 4 shows the variation of the normalized current with the applied bias voltage in a nanotube of length 24.5 Å. Here, the "normalized current" is defined as "the current obtained at different hopping integrals" divided
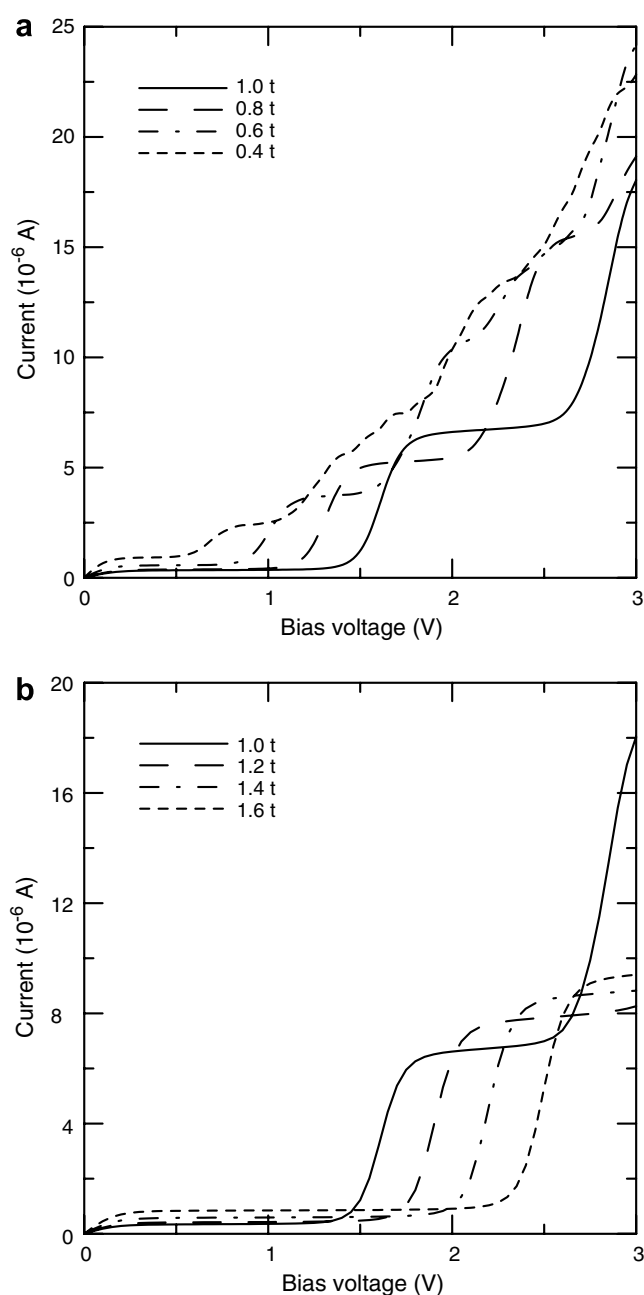
Fig. 3. Variation of current with bias voltage in zigzag nanotube of length 24.5 Å as function of hopping integral. (a) Shows the case of a decreasing hopping integral, while (b) shows the case of an increasing hopping integral.
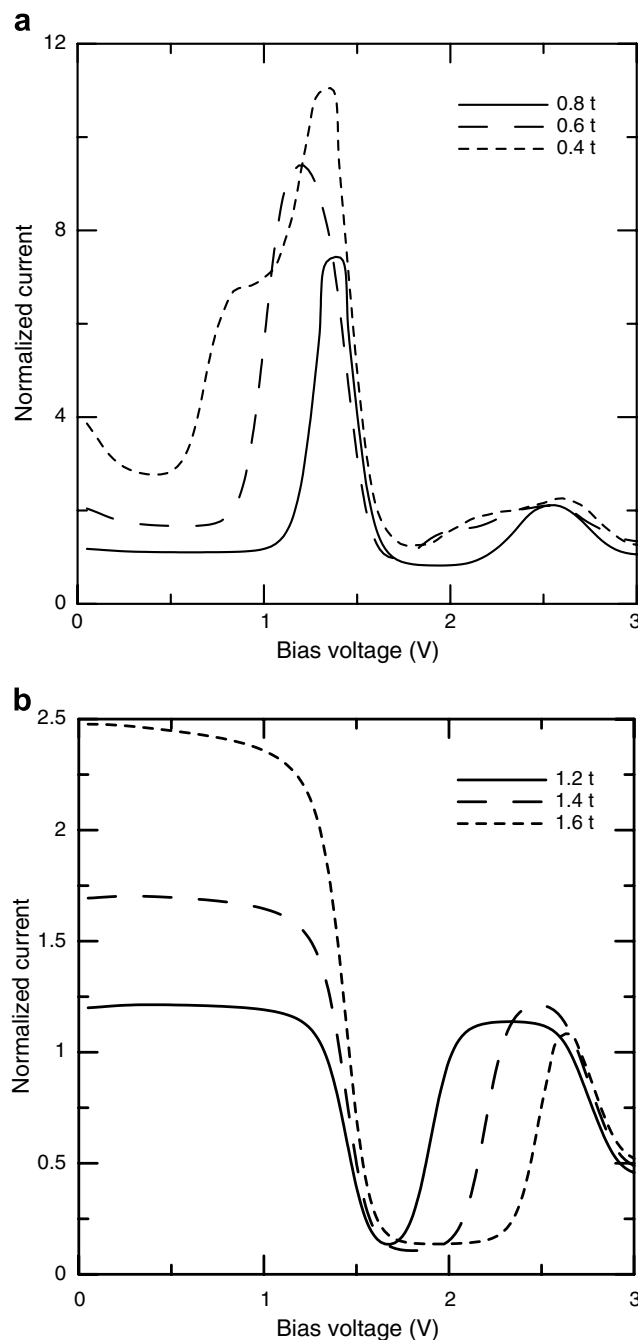

Fig. 4. Variation of normalized-current with bias voltage in zigzag nanotube of length 24.5 Å as function of hopping integral. (a) Shows the case of a decreasing hopping integral, while (b) shows the case of an increasing hopping integral.

by the "current obtained at the unit hopping integral $(1.0t)$". The unit hopping integral $(1.0t)$ [6] represents the hopping integral of nanotube without absorbing any molecule. In an experiment, the "sensitivity of operation" is a main feature of sensors, and it is obtained by dividing the current in the presence of polar molecules by that without absorbing any molecule. The normalized I–V profiles show at how much voltage the maximum sensitivity of operation appears. In Fig. 4a, which considers the case of a reducing hopping integral, it can be seen that the profiles have distinct peaks at voltages between 0.75 V and 1.5 V.

In this bias voltage range, the current increases by a factor of approximately 7–11 times, and the greatest increase is observed in the nanotube with the lowest hopping integral. Conversely, in Fig. 4b, which shows the case of an increasing hopping integral, the three profiles have pronounced troughs between 1.25 V and 2.5 V. In this bias voltage range, the current falls by a factor of approximately 10 times irrespective of the value of the hopping integral. In general, Fig. 4 confirms that an increasing hopping integral

reduces the maximum attainable current in the nanotube, while a decreasing hopping integral yields a significant increase in the current. Furthermore, it is observed that the widths of the peaks and troughs increase as the hopping integral decreases and increases, respectively.

To investigate the effect of the nanotube length on the electrical properties of the zigzag tube, Fig. 5 plots the *I–V* curves of a nanotube of length 41.8 Å at various values of the hopping integral. Fig. 5a shows that for a hopping integral of 0.4*t*, the first step in the profile virtually disap-

pears, while the other steps become less distinct. This effect arises because the intervals between the discrete energy states are more tightly compressed in a longer nanotube. As in the case of the shorter nanotube, it is observed that the voltage associated with the first step in the current profile increases as the hopping integral increases.

Fig. 6 shows the variation of the normalized current with the applied bias voltage in a nanotube of length 41.8 Å, and the normalized current is on a log scale. In Fig. 6a, the three current profiles have distinct peaks in
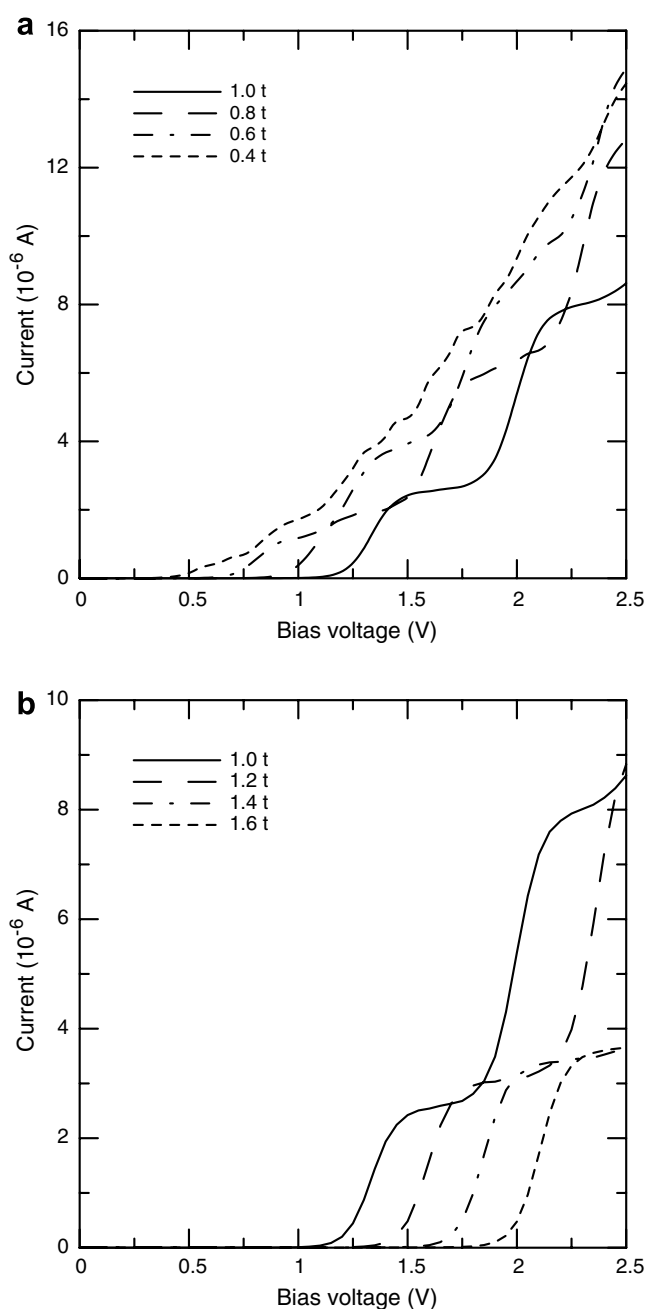

Fig. 5. Variation of current with bias voltage in zigzag nanotube of length 41.8 Å as function of hopping integral. (a) Shows the case of a decreasing hopping integral, while (b) shows the case of an increasing hopping integral.
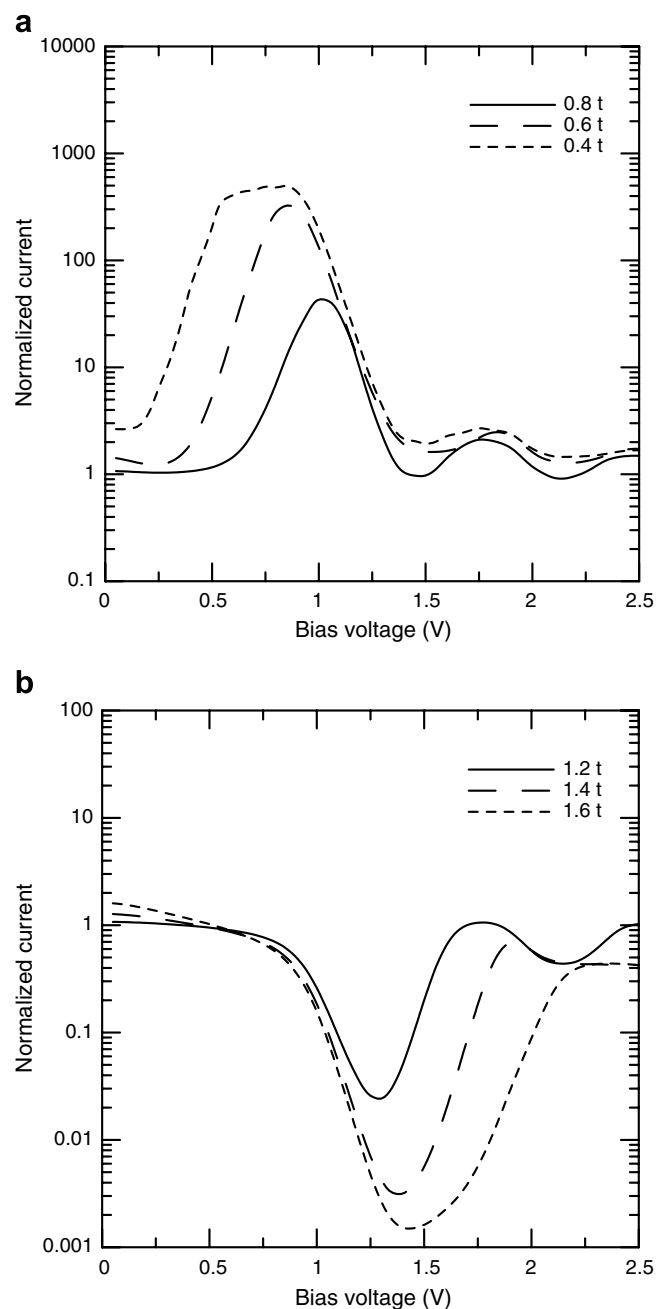
Fig. 6. Variation of normalized-current with bias voltage in zigzag nanotube of length 41.8 Å as function of hopping integral. (a) Shows the case of a decreasing hopping integral, while (b) shows the case of an increasing hopping integral.

the voltage range of 0.25 V–1.25 V. From inspection, it is found that the current in this voltage region increases by factors of 43, 326 and 497 times, respectively, for hopping integrals of 0.8*t*, 0.6*t* and 0.4*t*. Conversely, in Fig. 6b, the profiles have pronounced troughs at voltages between 0.75 V and 2.0 V. The currents in this voltage range reduce by factors of 0.024, 0.0032 and 0.0015 times that of their original values at hopping integrals of 1.2*t*, 1.4*t* and 1.6*t*, respectively. In contrast to the case of the shorter nanotube (Fig. 4b), the magnitude of the current reduction in the longer tube is strongly dependent on the value of the hopping integral. Specifically, the magnitude of the current reduction increases as the value of the hopping integral is increased. Furthermore, comparing Figs. 4 and 6, it is observed that in the longer zigzag nanotube, the peaks and troughs in the current-bias profile occur at a lower voltage.

The results presented in Figs. 3–6 suggest that zigzag nanotubes have the potential for use in ion or polar molecule sensing applications. When a nanotube, biased using an appropriate voltage, absorbs ions or polar molecules, a local electric field is produced in the tube and the ions or molecules hybridize with the host molecules. This causes a change in the hopping integral of the tube, which in turn changes the density of states, producing a detectable change in the current as a result. This study is also observed that the normalized *I–V* profiles exhibit more drastic increasing or decreasing in the longer zigzag nanotube. In general nanotube-based gaseous sensors, the tube lengths are typically of the order of several tens to hundreds of nanometers, and hence the nanotube conductance changes significantly for even slight changes in the hopping integral.

4. Conclusion

This study has performed a theoretical investigation into the electrical properties of zigzag carbon nanotubes with different hopping integrals. The results have shown that the *I–V* profiles have distinct steps at particular values of the bias voltage. These steps correspond to the bias voltage values at which the electrons are imparted sufficient energy to propagate through the nanotube. The normalized *I–V* profiles exhibit prominent peaks as the hopping integral decreases and distinct troughs as the hopping integral

increases. In longer nanotubes (41.8 Å), the current changes by several orders of magnitude in these regions of the *I–V* profiles and the peaks and troughs appear at lower bias voltages. In practice, the increasing or decreasing hopping integrals modeled theoretically in this study occur when ions or polar molecules are absorbed on the surface of the nanotube. Therefore, the present results suggest that a semi-conducting zigzag nanotube, with a suitable applied bias, can be used as an ion or molecule absorption sensor.

References

[1] Y. Xue, M.A. Ratner, Nanotechnology 16 (2005) 5.
[2] S. Dag, O. Gulseren, S. Ciraci, T. Yildirim, Appl. Phys. Lett. 83 (2003) 3180.
[3] A. Bachtold, P. Hadley, T. Nakanishi, C. Dekker, Science 294 (2001) 1317.
[4] V. Derycke, R. Martel, J. Appenzeller, P. Avouris, Nano Lett. 1 (2001) 453.
[5] S.J. Wind, J. Appenzeller, R. Martel, V. Derycke, P. Avouris, Appl. Phys. Lett. 80 (2002) 3817.
[6] R. Saito, G. Dresselhaus, M.S. Dresselhaus, Physical Properties of Carbon Nanotubes, Imperial College Press, 1998.
[7] Y. Hu, Y. Zhu, H. Gao, H. Guo, Phys. Rev. Lett. 95 (2005) 156803.
[8] G. Fagas, G. Cuniberti, K. Richter, Phys. Rev. B 63 (2001) 045416.
[9] S.H. Ke, H.U. Baranger, W. Yang, Phys. Rev. B 71 (2005) 113401.
[10] J. Kong, N.R. Franklin, C. Zhou, et al., Science 287 (2000) 622.
[11] Y.M. Wong, W.P. Kang, J.L. Davidson, et al., Sensors Actuators B 93 (2003) 327.
[12] J.K. Abraham, B. Philip, A. Witchurch, et al., Smart Mater. Struct. 13 (2004) 1045.
[13] J. Li, Y. Lu, Q. Ye, et al., Electrochem. Solid-State Lett. 8 (2005) H100.
[14] B.Y. Wei, M.C. Hsu, P.G. Su, et al., Sensors Actuators B 101 (2004) 81.
[15] S. Ghosh, A.K. Sood, N. Kumar, Science 299 (2003) 1042.
[16] S. Ghosh, A.K. Sood, S. Ramaswamy, N. Kumar, Phys. Rev. B 70 (2004) 205423.
[17] S. Ghosh, V. Gadagkar, A.K. Sood, Chem. Phys. Lett. 406 (2005) 10.
[18] Jijun Zhao, Alper Buldum, Jie Han, Jian Ping Lu, Nanotechnology 13 (2002) 195.
[19] Pil Sun Na, Hyojin Kim, Hye-Mi So, Ki-Jeong Kong, et al., Appl. Phys. Lett. 87 (2005) 093101.
[20] G. Grosso, G.P. Parravicini, Solid State Physics, Academic Press, 2000 (Chapter 1).
[21] V. Mujica, M. Kemp, M.A. Ratner, J. Chem. Phys. 101 (1994) 6849.
[22] X.Q. Li, Y.J. Yan, Appl. Phys. Lett. 79 (2001) 2190.
[23] M. Zwolak, M.D. Ventra, Appl. Phys. Lett. 81 (2002) 925.
[24] V.V. Dobrokhotov, C.A. Berven, Physica E 31 (2006) 160.
[25] WA. Harrison, Electronic Structure and the Properties of Solids, Dover, New York, 1989.